

## An approach for optimal sensor placement based on principal component analysis and sensitivity analysis under uncertainty conditions

Sahar Beygzadeh<sup>a</sup>, Peyman Torkzadeh\* and Eysa Salajegheh<sup>b</sup>

Departement of Civil Engineering, Shahid Bahonar University of Kerman, Kerman, Iran

(Received January 17, 2022, Revised March 17, 2022, Accepted April 3, 2022)

**Abstract.** In the present study, the objective is to detect the structural damages using the responses obtained from the sensors at the optimal location under uncertainty conditions. Reducing the error rate in damage detection process due to responses' noise is an important goal in this study. In the proposed algorithm for optimal sensor placement, the noise of responses recorded from the sensors is initially reduced using the principal component analysis. Afterward, the optimal sensor placement is obtained by the damage detection equation based sensitivity analysis. The sensors are placed on degrees of freedom corresponding to the minimum error rate in structural damage detection through this procedure. The efficiency of the proposed method is studied on a truss bridge, a space dome, a double-layer grid as well as a three-story experimental frame structure and the results are compared. Moreover, the performance of the suggested method is compared with three other algorithms of Average Driving Point Residue (ADPR), Effective Independence (EI) method, and a mass weighting version of EI. In the examples, young's modulus, density, and cross-sectional areas of the elements are considered as uncertainty parameters. Ultimately, the results have demonstrated that the presented algorithm under uncertainty conditions represents a high accuracy to obtain the optimal sensor placement in the structures.

**Keywords:** damage detection; optimal sensor placement; principal component analysis; sensitivity analysis; uncertainty

### 1. Introduction

Optimal sensor placement (OSP) is one of the essential criteria in Structural Health Monitoring (SHM) methods (Laory *et al.* 2012). SHM methods are combined with OSP techniques to perform several purposes: identify structural parameters, detect structural damages, and update the finite element model (He *et al.* 2014). Zhou *et al.* (2015a) presented the theoretical framework of optimal wireless sensor placement in SHM. In this study, the energy-aware wireless sensor placement was formulated as a discrete optimization problem and a Hybrid Discrete Firefly Algorithm (HDFA) was developed to solve this complex optimization algorithm. Yi *et al.* (2015) proposed a novel OSP algorithm called Adaptive Monkey Algorithm (AMA) to cope with the

---

\*Corresponding author, Associate Professor, E-mail: torkzadeh@uk.ac.ir

<sup>a</sup> Ph.D. Student

<sup>b</sup> Professor

sensor placement problem for target location under constraints of computing efficiency and convergence stability. In this method, a dual-structure coding method was used instead of the traditional coding method. Hosseini-Toudeshky and Amjad (2021) studied the optimization of sensor placement for SHM systems. In this study, attention was paid to the lamb wave or guided wave-based SHM. By using detection theory and the Bayes risk framework, the expected cost (loss) of decision making or Bayes risk to the SHM system was minimized and the optimal detector was obtained.

Structural damage detection using finite element model updating by evolutionary algorithms is an active research focus that is proceeding by researchers; but this subject lacks a comprehensive survey. To achieve this purpose, a review of the critical aspects of structural damage detection using the finite element model updating is presented (Alkayem *et al.* 2018). One of the major concerns in SHM is to infer the procedure of structural conditions from the responses and the responses collected from sensors. SHM's objectives are to detect structural damages with high accuracy, as well as to extend the useful life of structures. Ghiasi *et al.* (2016) proposed a new strategy for structural damage detection using least square support vector machines based on a new combinational kernel. Kaveh and Zolghadr (2015) formulated an approach for damage detection as an inverse optimization problem. In this approach, the amounts of damage to each element were considered as the optimization variables. The objective function was based on setting these variables such that the characteristics of the modal correspond to the experimentally measured characteristics of the actual damaged structure. Dinh-Cong *et al.* (2017) presented an efficient multi-stage optimization method for the damage detection in plate-like structures. In this method, the objective function was based on changes in the flexibility of the structure and a modified differential evolution algorithm was used for many stages of damage detection. Shyamala *et al.* (2018) proposed a damage detection method using the Support Vector Machine (SVM) algorithm that worked step by step by first locating and then determining the severity of the damage. The SVM algorithm uses simulations of only a limited number of damage scenarios and trains the algorithm in such a way that it detects damage at unknown locations by recognizing the pattern of changes in dynamic responses. In this study, a rectangular fiber reinforced plastic composite plate was investigated both numerically and experimentally to observe the efficiency of the SVM algorithm for damage detection. Khatir *et al.* (2019) presented a two-stage method for damage detection in beam-like structures. In this method, a new damage index was proposed to locate the damaged elements. Ghiasi *et al.* (2019) proposed an efficient three-stage method for damage detection of large-scale space structures by employing a forward substructuring approach, modal strain energy, and Enhanced Bat Algorithm (EBA) optimization. Ghannadi *et al.* (2020) studied the efficiency of grey wolf optimization algorithm for damage detection. In this study, the residual force vector based on expended mode shapes was considered as an objective function. Kahya *et al.* (2021) proposed automated model updating for the identification and location of damage in laminated composite beams. To simulate damage, the material moduli and the mass density of the beam were chosen as uncertain parameters and the sensitivity analysis was performed based on estimation of the Bayesian parameter. Crack locations were determined by evaluating changes in these parameters.

OSP techniques obtain a lower number of degrees of freedom (DOFs) to record the structural responses; therefore, the structural damage detection is achieved at a lower cost. In this regard, Kammer (1991) provided the Effective Independence (EI) method based on maximizing the determinant of the Fisher Information Matrix (FIM). In this method, the sensor positions were classified according to their contribution to the linear independence of the target modal partitions.

Iteratively, positions that do not contribute significantly to linear independence were eliminated. The FIM was also weighted with a mass matrix obtained from a finite element model. This research aimed to develop and investigate the use of an iterative Guyan expansion for mass weighting of target modes for OSP purposes (Kammer and Peck 2008). General methods for OSP often take advantage of dynamic parameters such as mode shapes and the natural frequencies. Researchers' trust was traditionally based on these methods and the finite element model analysis in the low frequency range. These methods are ineffective in the mid-frequency range due to the numerous mode shapes and high modal aggregation. In this aspect, a method for OSP was presented by Rao *et al.* (2014) in the mid frequencies. In the mentioned study, a typical procedure and a set of experimental data were considered to identify the modal parameters of the material. Since experimental results are usually affected by errors and are limited in number, it is essential to specify sensor locations to record the most informative data. Zhou *et al.* (2015b) adopted an uncertainty metric for the identified structural parameters as a performance measure for OSP. Also, OSP was formulated as the multi-objective optimization problem and the Nondirective Movement Glowworm Swarm Optimization (NMGSO) algorithm was proposed to identify the effective Pareto optimal sensor configurations. Yi *et al.* (2017) presented a holistic approach including a three-dimensional optimal criterion and solution method to find the optimal locations to implement triaxial sensors. In this approach, the three-dimensional optimal criterion was established by combining the three-dimensional modal guarantee criterion and the redundancy function. The Hierarchical Wolf Algorithm (HWA) was developed by mimicking the swarm intelligence embedded in the wolf pack to efficiently find the optimal triaxial sensor configuration with the proposed optimal three-dimensional criterion. Wang and Yang (2017) investigated the relationship between the error of damage identification and the sensitivity matrix. In this study, an index was defined according to the perturbation amplify effect, then an OSP method was proposed based on the minimization of that index. A novel method for OSP was presented by Chisari *et al.* (2017) that was based on the definition of the representativeness of the data with respect to the global displacement field. This method employed an optimization procedure based on the Genetic Algorithm (GA) and permitted any sensor layout assessment, regardless of the actual inverse problem solution. In another research, an OSP strategy was developed by Zhang *et al.* (2017) for multi-setup modal identification. As an optimality criterion, the information entropy was adopted in the stated research, which is a scalar measure of uncertainty in the Bayesian framework. Zhou *et al.* (2019) treated an optimal configuration of the wireless sensor network for structural health monitoring as a discrete optimization problem. They introduced a new swarm intelligence algorithm called machine learning firefly algorithm by integrating the original firefly algorithm with the Lévy flight and machine learning mechanism to solve this optimization problem. A useful function was provided by Dinh-Cong *et al.* (2018) for OSP and damage detection in laminated composite structures. In this role, the space required to optimize sensor placement was initially reduced through an Iterated Improved Reduced System (IIRS) method. Afterward, the OSP problem was solved by Jaya's algorithm. The objective function was defined from the correlation between the flexibility matrix obtained from an original finite element model and the corresponding matrix calculated from the IIRS. A robust method was proposed by Yang *et al.* (2018) for OSP under uncertainty conditions. The non-probability performance was used to avoid creating errors in incomplete data. In this research, the FIM was obtained based on the modal analysis. Additionally, an unbiased state of several studies in the area of optimal sensor placement for SHM applications was presented by Ostachowicz *et al.* (2019). In the mentioned research, at first, the definition of the OSP problem was presented; subsequently, each step of the optimization

was described. On the other hand, Tan and Zhang (2020) investigated a comprehensive review of computational methodologies for OSP. In this review, the formulation of the OSP issue was initially introduced; subsequently, various existing optimization methodologies were summarized and introduced in detail; specifically, evolutionary algorithms and their improved variants were examined. In one of the studies, a procedure to select an optimal number of sensor placement based on a comparison between the probability of damage occurrence and the probability of detecting damage was suggested by Lofrano *et al.* (2020). In this paper, the non-localized damage was described using a Gaussian distributed random damage parameter. Liu *et al.* (2020) proposed a sensor placement framework based on the Deflection Influence Line (DIL) analysis for the optimal design of damage detection-oriented BHM system. They explored the change of global stiffness matrix, damage coefficient matrix and DIL vector caused by structural damage to improve damage detection accuracy. They developed a new sensor placement framework based on the Fisher information matrix.

Shi *et al.* (2020) proposed an OSP method based on a Weighted Standard Deviation Norm (WSDN) index. In this study, the OSP procedure was performed by minimizing the WSDN index. Other OSP criteria, including condition number, information entropy, and standard deviation norm were analyzed in this paper for comparison with the proposed method. Altunisik *et al.* (2021) investigated the OSP for dynamic characteristics identification of arch dams. For this purpose, a prototype arch dam was constructed in laboratory conditions. In this study, enhanced frequency domain decomposition and stochastic subspace identification methods were used to extract experimental dynamic characteristics and the OSP were specified using the effective independence method. Das and Dhang (2022) presented a damage detection method based on efficient multi-stage optimization method with a limited number of sensors. In this method, a finite element model was developed to simulate the response of the actual structure. The limited sensor condition for this finite element model was obtained by the modal reduction method.

Researchers have considered the uncertainty of structural parameters in OSP and the damage detection process in recent years. The uncertainty on structural parameters is considered as the difference between the actual physical parameters of structures and the categories of the structural analysis. In most cases, finding a solution for the OSP issue is challenging as it requires performing an optimization procedure under the mentioned uncertainties. In this aspect, a novel algorithm was developed for OSP under uncertainty conditions in a reliable monitoring system by Pourali and Mosleh (2013). The effects of the uncertainty parameters in the OSP techniques were investigated for structural modal analysis by Castro-Triguero *et al.* (2013). In another study, the role of modeling errors and uncertainty parameters were examined in sensor placement optimization (or nearly optimization) for SHM and modal tests by Vincenzi and Simonini (2017). Furthermore, Kim *et al.* (2018) introduced a stochastic EI method for OSP under uncertainty conditions. This method reported to have the best linear independence of the structural mode shapes. In another research, an assessment-guided optimal sensor placement algorithm was proposed based on the least mean square root by Liu *et al.* (2018). The results of this algorithm demonstrated that the obtained OSP algorithm contained the best orthogonality of mode shapes.

In the present study, a novel method for OSP is proposed based on noise reduction in the responses recorded from the sensors in uncertainty conditions. Initially, the effect of noise on the response of the sensors is reduced by Principal Component Analysis (PCA) method. Afterward, the OSP is determined by reducing errors in the damage detection process. The OSP problem is considered a numerical problem. For this purpose, the damage detection equation based on sensitivity analysis is geometrically considered as a linear mapping of the response changes space

to the damaged space. Therefore, the existing noise of the recorded responses of the sensors is mapped to the damaged space; therefore, the accuracy of the damage detection process is reduced. In the proposed method, OSP aims to map the minimum noise level to the damaged space and increase the accuracy of the damage detection process.

The sensitivity analysis for the damage detection problem is investigated in Section 2 of the current paper, and the principal component analysis is briefly illustrated in Section 3. Furthermore, the study's novel OSP algorithm is proposed in Section 4, and three criteria for evaluating the OSP are offered in Section 5. Finally, Section 6 investigates the numerical results of the proposed method for a truss bridge, a space dome and a double-layer grid. In addition, the proposed method is validated by a three-story and two-bay experimental frame structure. The conclusions of the study are presented in the last section.

## 2. Sensitivity Analysis (SA)

The damage causes changes in the responses recorded from sensors in the structures. The response vector in the damaged structure is a nonlinear function of the damage vector. Therefore, the problem of damage detection is defined as follows

$$\boldsymbol{\phi}_d = \boldsymbol{\phi}(\mathbf{Z}), \quad \mathbf{Z} = \{z_1, z_2, \dots, z_n\}^T \quad 0 \leq z_i \leq 1 \quad (1)$$

where  $\mathbf{Z}$  is the damage vector, and  $n$  represents the number of structural elements. The values of  $z_i = 0$  and  $z_i = 1$  indicate the damage rate of  $i$ th element in healthy and damaged states, respectively. The vector  $\boldsymbol{\phi}_d = \{\phi_{d1}, \phi_{d2}, \dots, \phi_{dm}\}^T$  is the structural response vector to the existing damage and  $\boldsymbol{\phi}(\mathbf{Z}) = \{\phi_1(\mathbf{Z}), \phi_2(\mathbf{Z}), \dots, \phi_m(\mathbf{Z})\}^T$  is the structural response vector to hypothetical damages at  $m$  DOFs in which the sensors are placed; this vector can be obtained from the analytical model of the structure. In this study, the eigenvectors in the target modes are used as structural responses in the damage detection problem.

To solve Eq. (1), the Taylor expansion  $\boldsymbol{\phi}(\mathbf{Z})$  is used as follows

$$\boldsymbol{\phi}_d = \boldsymbol{\phi}_h + \frac{\partial \boldsymbol{\phi}}{\partial \mathbf{Z}} \Delta \mathbf{Z} + \dots \quad (2)$$

In this equation,  $\boldsymbol{\phi}_h$  is an indicator of the eigenvector of the healthy structure. Using the first two components of the Taylor expansion, Eq. (2) is expressed as

$$\Delta \boldsymbol{\phi} = \boldsymbol{\phi}_d - \boldsymbol{\phi}_h = \frac{\partial \boldsymbol{\phi}}{\partial \mathbf{Z}} \Delta \mathbf{Z}, \quad \mathbf{S} = \frac{\partial \boldsymbol{\phi}}{\partial \mathbf{Z}} \quad \Rightarrow \quad \Delta \boldsymbol{\phi} = \mathbf{S} \cdot \Delta \mathbf{Z} = \mathbf{S}(\mathbf{Z} - \mathbf{Z}_0) \quad (3)$$

where  $\mathbf{Z}_0$  is damage vector of the healthy structure, so it is a zero vector, and  $\mathbf{S}$  is the sensitivity matrix (Naserlavi *et al.* 2010).

## 3. Principal Component Analysis (PCA)

Due to existing the error probability derived from the visibility or failure of the sensors, the data recorded from the sensors is generally noisy. One of the methods to reduce the mentioned

noise is to apply the Principal Component Analysis (PCA) method. PCA is a general mathematical technique that is widely applied to analyze data set problems. PCA was initially introduced by Pearson (1901). In this method, an orthogonal space of target data is acquired to transmit initial data to a new cross-correlations coordinate system. After the PCA transfer, the orthogonal space is divided into two sub-spaces: the main and noisy sub-spaces. To obtain the indicated principal and noisy sub-spaces, the covariance matrix is utilized. The principal components of the PCA space are called pcs, and these components correspond to the largest eigenvalues of the covariance matrix that are orthogonal and non-relevant. The matrix has been assumed to represent the recorded responses of  $m$  sensors on the damaged structure  $\boldsymbol{\phi}_d$  as follows

$$\boldsymbol{\phi}_d = \begin{bmatrix} \phi_{11d} & \cdots & \phi_{1pd} \\ \vdots & \ddots & \vdots \\ \phi_{m1d} & \cdots & \phi_{mpd} \end{bmatrix} = [\boldsymbol{\phi}_{1d} \quad \boldsymbol{\phi}_{2d} \quad \cdots \quad \boldsymbol{\phi}_{pd}], \quad \boldsymbol{\phi}_{jd} = [\phi_{1jd} \quad \phi_{2jd} \quad \cdots \quad \phi_{mjd}]^T \quad (4)$$

where  $\phi_{ij_d}$  is the  $i$ th component of the eigenvector in the  $j$ th mode in the damaged structure, and  $p$  represents the number of target modes. To apply PCA,  $\bar{m}_i$  which is indicator of the average of data recorded from the sensors in the  $i$ th DOF, is initially calculated

$$\bar{m}_i = \frac{1}{p} \sum_{j=1}^p \phi_{ij_d} \quad (5)$$

The normalized matrix of  $\boldsymbol{\phi}_d$ , which is called  $\mathbf{D}$  matrix, is as follows

$$\mathbf{D} = \begin{bmatrix} d_{11} & \cdots & d_{1p} \\ \vdots & \ddots & \vdots \\ d_{m1} & \cdots & d_{mp} \end{bmatrix}, \quad d_{ij} = \phi_{ij_d} - \bar{m}_i \quad (6)$$

Furthermore, the covariance matrix of the normalized data is obtained according to the following equation

$$\mathbf{C} = \frac{1}{p-1} \mathbf{D}\mathbf{D}^T \quad (7)$$

Eigenvalues and eigenvectors of the  $\mathbf{C}$  matrix are obtained, and the eigenvectors corresponding to the largest value are the same as pcs (Hotelling 1993). In this study, the pcs obtained from the responses of the damaged structure contain the largest variance and, therefore, retain the essential information of  $\boldsymbol{\phi}_d$  matrix. The maximum variance contains the first few principal components, while the remaining less essential components include the measurement noise (Zhang *et al.* 2019). In this study, the number of principal components to take in the analysis is considered  $m$ .

#### 4. The proposed algorithm for the OSP based on Principal Component Analysis and Sensitivity Analysis (PCA-SA)

There is a challenging problem in the damage detection process that due to the noise in the recorded structural responses from the sensors and the limited number of sensors, the damage

detection results are often not accurate. In this sense, if a sufficient amount of data is used in the damage detection process, the accuracy of the detected damages will increase.

According to Eq. (3), the damage is obtained as follows

$$\Delta \mathbf{Z} = \mathbf{S}^+ \cdot (\Delta \boldsymbol{\phi} + \vartheta) \quad (8)$$

where  $\mathbf{S}^+$  is pseudo-inverse of the sensitivity matrix, and  $\vartheta$  is a noise vector that has a normal Gaussian distribution. In this study, a normal distribution of the noise vector with zero mean and covariance matrix of  $\mathbf{I}_{m \times m}$  is considered. This noise is geometrically considered as a sphere unit.

Mathematically, in any linear equation such as  $\mathbf{A} \cdot \mathbf{x} = \mathbf{b}$ , the matrix  $\mathbf{A}$  maps the vector space  $\mathbf{x}$  to the vector space  $\mathbf{b}$ . Similarly, in Eq. (3), the matrix  $\mathbf{S}$  maps the vector space  $\Delta \mathbf{Z}$  (called  $\Delta \mathbf{Z}$  space) to the vector space  $\Delta \boldsymbol{\phi}$  (called  $\Delta \boldsymbol{\phi}$  space). By Eq. (8), the pseudo-inverse matrix,  $\mathbf{S}^+$ , will inverse result in an inverse mapping from space  $\Delta \boldsymbol{\phi}$  to the space  $\Delta \mathbf{Z}$ . The normal noise covariance matrix  $\mathbf{I}$  in space  $\Delta \boldsymbol{\phi}$  with inverse mapping changes to the covariance matrix of  $\mathbf{S}^+ \cdot \mathbf{I} \cdot \mathbf{S}^{+T}$  in the space  $\Delta \mathbf{Z}$ . This noise is geometrically considered as an ellipsoid. If the volume of this ellipsoid decreases in the space  $\Delta \mathbf{Z}$ , the damage detection results will be equal to a more accurate value. Therefore, the sensors should be placed on DOFs where the mapped noise of the  $\Delta \mathbf{Z}$  space becomes minimum (Beygzadeh *et al.* 2014). The OSP problem can be expressed as follows

$$\begin{aligned} &\text{Minimize} && \text{Volume} \left( \mathbf{S}^+ \cdot \mathbf{I} \cdot \mathbf{S}^{+T} \right) \\ &\text{subject to} && |\bar{\mathcal{S}}| = ns \end{aligned} \quad (9)$$

where  $\bar{\mathcal{S}} \equiv \{i, i \in NDOF\}$  is a set of sensors;  $NDOF$  represents the total number of DOFs that can be replaced by sensors, and  $ns$  is the number of available sensors. The symbol  $|\bar{\mathcal{S}}|$  is the size of the set  $\bar{\mathcal{S}}$ . Since the properties of a pseudo-inverse matrix are benefit, then the optimization problem can be expressed as

$$\begin{aligned} &\text{Minimize} && \text{Volume} (\mathbf{S} \cdot \mathbf{I} \cdot \mathbf{S}^T) \\ &\text{subject to} && |\bar{\mathcal{S}}| = ns \end{aligned} \quad (10)$$

According to Eq. (10), the set  $\bar{\mathcal{S}}$  is chosen from the DOFs corresponding to the largest volume of covariance matrix  $\mathbf{S} \cdot \mathbf{I} \cdot \mathbf{S}^T$  in space  $\Delta \boldsymbol{\phi}$ . If the covariance ellipsoid has the largest volume in space  $\Delta \boldsymbol{\phi}$ , this projection of covariance on any vector of space  $\Delta \boldsymbol{\phi}$  has the most significant value. Therefore, the space  $\Delta \boldsymbol{\phi}$  consists of some DOFs found by using the optimization problem. The projection of the covariance ellipsoid in this space has the highest value. Hence, the optimization problem in Eq. (10) is expressed as follows

$$\begin{aligned} &\text{Maximize} && \text{proj}_{\bar{\mathcal{S}}} \mathbf{S} \cdot \mathbf{I} \cdot \mathbf{S}^T \\ &\text{subject to} && \hat{\mathcal{S}} = [e_1, e_2, \dots, e_{ns}] \end{aligned} \quad (11)$$

where  $e_i$  represents a unit vector for the  $i$ th vector of the space  $\Delta \boldsymbol{\phi}$ , in which the  $i$ th element is equal to one and the other elements are zero. Moreover,  $ns$  indicates the number of available sensors. The projection of the covariance matrix is obtained from the following equation

$$\text{proj}_{\bar{\mathcal{S}}} \mathbf{S} \cdot \mathbf{I} \cdot \mathbf{S}^T = \hat{\mathcal{S}} \cdot \hat{\mathcal{S}}^{-1} \cdot \mathbf{S} \cdot \mathbf{I} \cdot \mathbf{S}^T \quad (12)$$

The optimization problem in the Eq. (11) is considered a numerical problem. The projection of a covariance matrix in any DOF is calculated according to Eq. (12). The DOFs are sorted corresponding to the decreasing projection values.

In the present study, uncertainty conditions are simulated using the Monte Carlo simulation (Robert and Casella 2010). Monte Carlo simulation (MCS) requires a large number of simulations and high computational costs. In this paper, the uncertainty parameters are introduced into the Monte Carlo method by taking 1000 analysis samples; furthermore, the computational cost or time for structural analysis is also considered appropriate. In this sense, Young's modulus, density, and cross-sectional area of the elements vary in each sample.

In this regard, the proposed OSP algorithm which is called PCA-SA is presented as follows:

Set  $i = 1$ , the number of simulations ( $iteration = 1000$ ), the number of target modes ( $p$ ), the number of available sensors ( $ns$ )

**Repeat**

Consider uncertainty parameters:  $A_i, \rho_i, E_i$

Model the structure and perform modal analysis by OpenSees software

Calculate the OSP using PCA-SA algorithm

---

**PCA-SA algorithm**

---

Set  $j = 1$ , the number of DOFs ( $m$ ), Q and G vectors with the number of  $m \times 1$  size

Select  $p$  eigenvectors

Impose measurement noise to eigenvectors

Reduce the noise using PCA method

**Repeat**

Calculate matrix S and  $f_i = \mathbf{proj}_S \mathbf{I} \cdot \mathbf{S}^T$  using Eq. (12)

Increase  $j$  by one unit

**Until**  $j = m$

$Q_i =$  The values  $f_i$  arranged in a decreasing order

$G_i =$  The DOF corresponding to  $Q_i$

OSP =  $G_1$  to  $G_{ns}$

---

Increase  $i$  by one unit

**Until**  $i = iteration$

Compute the possibility of selecting each DOF as the OSP in samples

Select the DOFs with the most repeated OSP possibility

## 5. Assessment criteria

To evaluate the results of the proposed algorithm for optimal sensor placement, three criteria have been considered:

### 5.1 Fisher Information Matrix (FIM)

This algorithm aims to find the best DOFs that maintain linear independence between the mode shapes. Initially, the modal matrix is derived from the complete finite element model. Since all the responses of all DOFs of a finite element model cannot be measured; therefore, the rotational DOFs and the degrees that cannot be measured are eliminated from the modal matrix. Similarly, all

the mode shapes cannot be measured empirically, as well; therefore, a series of target mode shapes are chosen optimally. Since each row in the modal matrix corresponds to one degree of freedom, some DOFs (rows) are preserved. In the full modal matrix, the columns corresponding to the target mode shapes are kept. Consequently, the Fisher information matrix is defined as follows

$$FIM = \boldsymbol{\phi}^T \boldsymbol{\phi} \quad (13)$$

If the determinant of the FIM matrix is zero, the columns of the modal matrix will be linearly dependent. Therefore, this method aims to select the best DOFs that maximize the determinant of the FIM matrix (Castro-Triguero *et al.* 2013).

### 5.2 Modal Assurance Criterion (MAC)

In general, the purpose of this criterion is to achieve a relationship between  $\boldsymbol{\phi}_i$  and  $\boldsymbol{\phi}_j$  mode shapes. The components of the MAC matrix are (Castro-Triguero *et al.* 2013)

$$MAC_{ij} = \frac{(\boldsymbol{\phi}_i^T \boldsymbol{\phi}_j)^2}{(\boldsymbol{\phi}_i^T \boldsymbol{\phi}_i)(\boldsymbol{\phi}_j^T \boldsymbol{\phi}_j)} \quad (14)$$

If an element of this matrix is zero, the vectors  $\boldsymbol{\phi}_i$  and  $\boldsymbol{\phi}_j$  will be uncorrelated, and if the value is one, the two modes will be completely correlated. In this paper, the MAC matrix is calculated in some DOFs. Therefore, the diagonal components of this matrix are always one, and the others are between zero and one. The best sensor placement has the lowest values for off-diagonal components. To obtain a qualitative measurement of the sensors, the root mean square (RMS) can be obtained for off-diagonal elements of the matrix.

$$RMS = \sqrt{\frac{1}{p(p-1)} \sum_{i=1}^p \sum_{\substack{j=1 \\ j \neq i}}^p (MAC_{ij})^2}, \quad i = 1, \dots, p, \quad j = 1, \dots, p \quad (15)$$

where  $p$  represents the number of target modes. The value of this parameter for a suitable sensor placement gains a lower value than the other sensor placements (Castro-Triguero *et al.* 2013).

### 5.3 Singular Value Decomposition ratio (SVD)

In the modal matrix of the structure, the special values can be divided as (Castro-Triguero *et al.* 2013)

$$\boldsymbol{\phi}_{m \times p} = \mathbf{U}_{m \times p} \bar{\mathbf{P}}_{p \times p} \mathbf{V}_{p \times p}^T \quad (16)$$

The matrix  $\bar{\mathbf{P}}$  is a diagonal matrix, in which the elements of the main diagonal are the eigenvalues obtained from the modal matrix. If the mode shape vectors are linearly dependent; thus, there is at least one zero value in the eigenvalues. To compare the obtained sensor placements, the smallest value of the largest values in the eigenvalues represents the best sensor position.

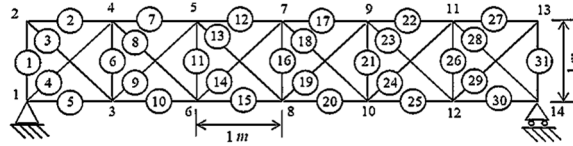


Fig. 1 31-bar truss bridge

Table 1 Active DOFs in truss bridge

Node	Horizontal DOF	Vertical DOF	Node	Horizontal DOF	Vertical DOF
2	1	2	9	15	16
3	3	4	10	17	18
4	5	6	11	19	20
5	7	8	12	21	22
6	9	10	13	23	24
7	11	12	14	25	-
8	13	14			

## 6. Numerical results

In this section, a truss bridge, a space dome, and a double-layer grid are considered and studied. In order to evaluate the efficiency of the proposed method for OSP, the obtained results are compared with the results of three other algorithms, including Average Driving Point Residue (ADPR), Effective Independence (EI) method, and a mass weighting version of EI (EI-mass) (Liu *et al.* 2018). In addition, the three comparative criteria described in Section 5 are evaluated, and the results of the algorithms are compared with each other. In this study, a noise level of 5% is imposed on the mode shapes of the structures.

### 6.1 Truss bridge

The truss bridge presented in Fig. 1 has 31 members, 14 nodes, and 25 DOFs (Castro-Triguero *et al.* 2013). The active DOFs in this truss have been shown in Table 1.

In this example, the first ten modes are used to form the modal matrix. A normal distribution of Young's modulus, density, and cross-sectional area of members are considered the uncertainty parameters. The mean and distribution of the uncertainty parameters are presented in Table 2 (Castro-Triguero *et al.* 2013).

Table 2 Uncertainty parameters

Parameter	Mean	Covariance
Young's modulus (GPa)	70	8
Mass density (kg/m <sup>3</sup> )	2800	4
Cross-sectional area (m <sup>2</sup> )	0.0025	5

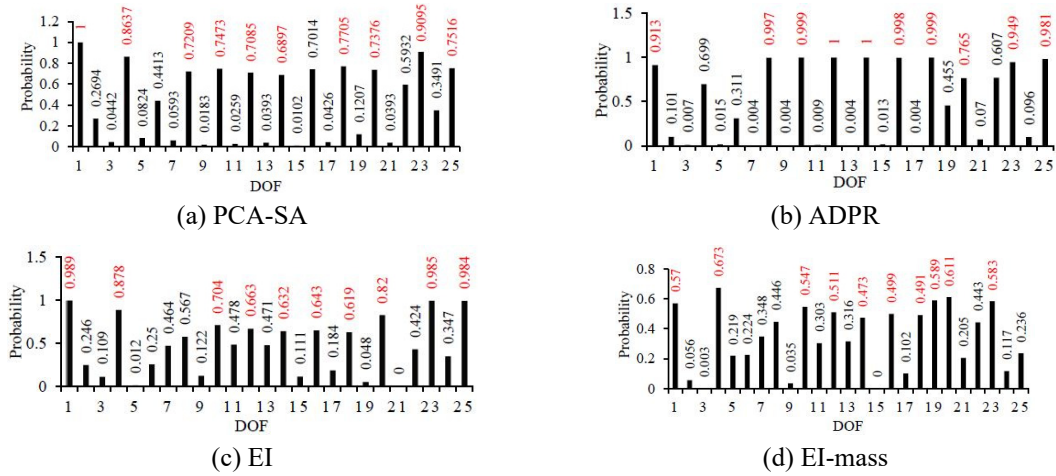


Fig. 2 Probability of the sensor placement

Table 3 DOFs corresponding to the optimal sensor placement

Algorithm	DOF									
PCA-SA	1	4	8	10	12	14	18	20	23	25
ADPR	1	8	10	12	14	16	18	20	23	25
EI	1	4	10	12	14	16	18	20	23	25
EI-mass	1	4	10	12	14	16	18	19	20	23

Table 4 Assessment criteria for the obtained sensor placement

Criteria	Algorithm			
	PCA-SA	ADPR	EI	EI-mass
FIM	4.65E+0.4	3.68E+0.4	3.56E+0.4	2.97E+0.4
RMS	0.0577	0.0727	0.0613	0.0614
SVD	0.041	0.0088	0.04	0.04

In this structure, it is assumed that there are ten sensors available. The probability of choosing each degree of freedom as one of the ten sensor positions is shown in Fig. 2. According to these figures, ten optimal sensor placement with the highest probability has been shown in Table 3.

For each position obtained from Table 3, the three assessment criteria are calculated and demonstrated in Table 4.

According to Table 4, the FIM value obtained by the PCA-SA algorithm is higher than the other algorithms; therefore, this algorithm maintains linear independence between the mode shapes. In addition, the RMS value obtained by the PCA-SA algorithm is lower than the other algorithms, indicating that the off-diagonal elements of the MAC matrix have the lowest value in this algorithm. Moreover, the SVD values obtained by PCA-SA, EI, and EI-mass are almost similar and are higher than the ADPR value. Finally, the results reveal that the accuracy of PCA-SA is considerably better

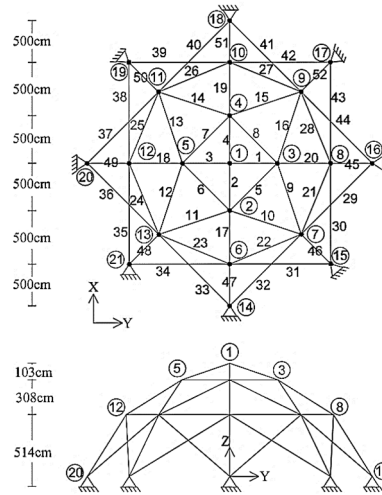


Fig. 3 52-bar space dome

Table 5 Active DOFs in space dome

Node	DOF in X-direction	DOF in Y-direction	DOF in Z-direction	Node	DOF in X-direction	DOF in Y-direction	DOF in Z-direction
1	1	2	3	8	22	23	24
2	4	5	6	9	25	26	27
3	7	8	9	10	28	29	30
4	10	11	12	11	31	32	33
5	13	14	15	12	34	35	36
6	16	17	18	13	37	38	39
7	19	20	21				

than the other algorithms. Furthermore, the effect of noise on the responses recorded from sensors is less than the other algorithms.

## 6.2 Space dome

A 52-bar space dome is considered according to Fig. 3. The elements of this steel structure represent the following characteristics: Young's modulus  $E = 70$  GPa; density  $\rho = 2770$  kg / m<sup>3</sup>; and cross-sectional area  $A = 0.0050$  m<sup>2</sup> (Beygzadeh *et al.* 2014).

This structure has 21 nodes and each node has three DOFs. The active DOFs corresponding to each node are shown in Table 5. The DOFs of nodes 14, 15, 16, 17, 18, 19, 20, and 21 are constrained; It is worth mentioning that the structure has 39 active DOFs.

In this structure, the first ten modes are employed to form the modal matrix. The normal distribution characteristics for the uncertainty parameters are given in Table 6.

It is assumed that 12 sensors are available. The probability of choosing each degree of freedom as one of the 12 sensor positions is shown in Fig. 4. According to these figures, 12 optimal sensor positions are the DOFs with the maximum probability presented in Table 7. For each position

Table 6 Uncertainty parameters

Parameter	Mean	Covariance
Young's modulus, GPa	70	8
Mass density, kg/m <sup>3</sup>	2770	4
Cross-sectional area, m <sup>2</sup>	0.005	10
Cross-sectional area, m <sup>2</sup>	0.005	10

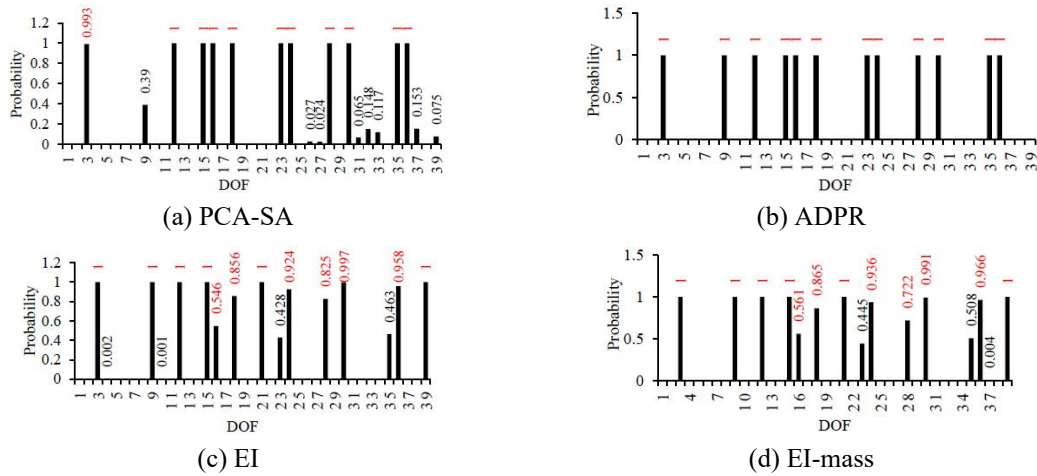


Fig. 4 Probability of the sensor placement

Table 7 DOFs corresponding to the optimal sensor placement

Algorithm	DOF					
PCA-SA	3	9	12	15	16	18
	23	24	28	30	35	36
ADPR	3	9	12	15	16	18
	23	24	28	30	35	36
EI	3	9	12	15	16	18
	21	24	28	30	36	39
EI-mass	3	9	12	15	16	18
	21	24	28	30	36	39

Table 8 Assessment criteria for the obtained sensor placement

Criteria	Algorithm			
	PCA-SA	ADPR	EI	EI-mass
FIM	4.16E+0.4	4.16E+0.4	1.64E+0.4	1.64E+0.4
RMS	0.0102	0.0102	0.0102	0.0102
SVD	0.2101	0.2101	0.2098	0.2098

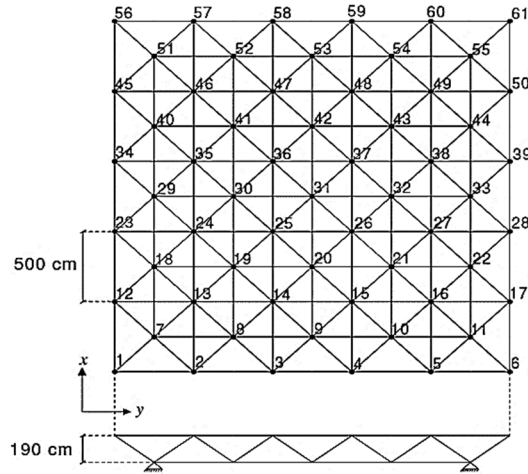


Fig. 5 200-bar double layer grid

obtained from Table 7, the three assessment criteria are evaluated and displayed in Table 8.

According to Table 7, the OSPs obtained by the PCA-SA and ADPR algorithms are similar. A comparison of the FIM value in Table 8 indicates that the optimal sensor placements obtained by the PCA-SA and ADPR algorithms are more accurate than the EI and EI-mass algorithms. The mentioned point reflects that the PCA-SA and ADPR algorithms better maintain the linear independence between the mode shapes than other algorithms. In this example, the RMS value in all algorithms is similar; therefore, this criterion is not suitable for comparing the evaluated algorithms of this example. Moreover, the SVD value obtained by PCA-SA and ADPR is higher than the other algorithms. Ultimately, the results of the proposed algorithm are suitable for OSP.

### 6.3 Double-layer grid

In this section, a 200-bar double-layer grid shown in Fig. 5 is considered. The characteristics of the elements of this steel structure are: Young's modulus  $E = 20$  GPa; and density  $\rho = 2770$  kg / m<sup>3</sup> (Beygzadeh *et al.* 2014).

This structure has 61 nodes, and each node has three DOFs. The DOFs of nodes 7, 11, 51, and 55 are constrained; Moreover, the structure has 171 active DOFs. In this structure, 20 modes are employed to form the modal matrix. The normal distribution characteristics for the uncertainty parameters are given in Table 9.

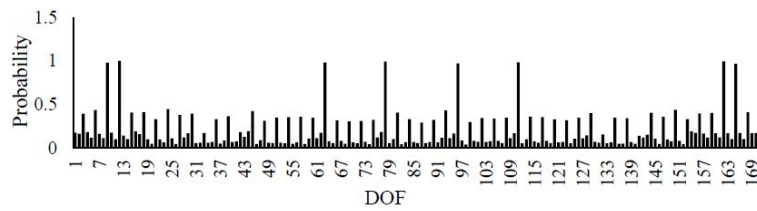
It is assumed that 30 sensors are available. The probability of choosing each degree of freedom as one of the 30 positions of sensors is obtained from Fig. 6. Within these figures, 30 sensor positions with the highest probability are considered optimal, which are shown in Table 10.

Table 9 Uncertainty parameters

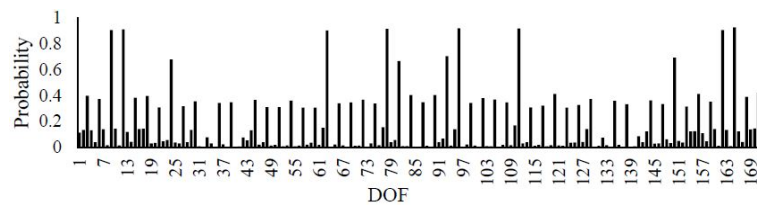
Parameter	Mean	Covariance
Young's modulus, GPa	20	8
Mass density, kg/m <sup>3</sup>	2770	4

Table 10 DOFs corresponding to the optimal sensor placement

Algorithm	DOF						
PCA-SA	3	6	9	12	15	18	24
	27	30	39	45	57	63	78
	81	93	96	111	114	117	129
	144	147	150	156	159	162	165
	171	168					
ADPR	3	6	9	12	15	18	24
	45	54	63	69	72	78	81
	84	90	93	96	102	105	111
	120	129	144	150	156	162	165
	168	171					
EI	3	6	9	12	15	18	36
	42	51	57	60	63	69	75
	78	81	84	90	96	102	108
	111	117	123	126	129	135	141
	150	171					
EI-mass	6	9	12	15	36	42	45
	51	60	69	72	75	78	81
	84	90	93	96	102	105	108
	111	114	117	126	135	141	144
	150	171					

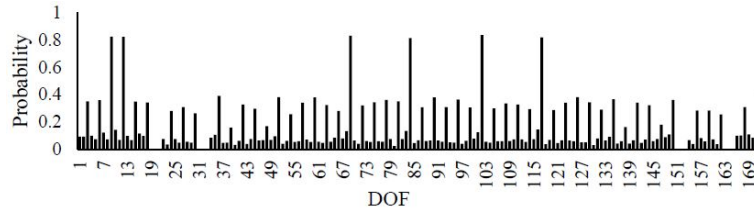


(a) PCA-SA

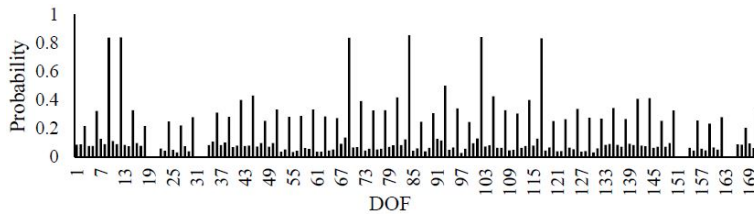


(b) ADPR

Fig. 6 Probability of the sensor placement



(c) EI



(d) EI-mass

Fig. 6 Continued

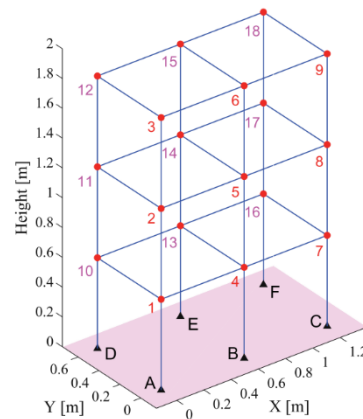
Table 11 Assessment criteria for the obtained sensor placement

Criteria	Algorithm			
	PCA-SA	ADPR	EI	EI-mass
FIM	5.871e+13	4.452e+13	1.635e+13	3.688e+12
RMS	0.0136	0.016	0.0153	0.0241
SVD	0.116	0.103	0.0915	0.0660

A comparison of the results obtained by the PCA-SA, ADPR, EI, and EI-mass algorithms, in Table 11 illustrates that the OSP obtained by PCA-SA is more accurate than the other mentioned algorithms.



(a) Experimental spatial frame



(b) Finite element model

Fig. 7 A three-story experimental frame structure

Table 12 Active DOFs in spatial frame

Node	DOF in X-direction	DOF in Y-direction	Node	DOF in X-direction	DOF in Y-direction	Node	DOF in X-direction	DOF in Y-direction
1	1	2	7	13	14	13	25	26
2	3	4	8	15	16	14	27	28
3	5	6	9	17	18	15	29	30
4	7	8	10	19	20	16	31	32
5	9	10	11	21	22	17	33	34
6	11	12	12	23	24	18	35	36

Table 13 Uncertainty parameters

Parameter	Mean	Covariance
Young's modulus, GPa	196	8
Cross-sectional area, cm <sup>3</sup>	38.71	4

#### 6.4 Three-story experimental frame structure

Sun and Büyüköztürk (2015) studied a three-story and two-bay experimental steel frame at the MIT structural laboratory to validate the OSP performance in SHM. This experimental spatial frame and its finite element model is shown in Fig. 7. The structure consists of 39 elements and 24 nodes that the bottom nodes at the base are fixed. Each element of this frame has dimensions  $5.08 \times 0.635 \times 60.96$  cm. The characteristics of the elements are: Young's modulus  $E = 196$  GPa; and density  $\rho = 7880$  kg/m<sup>3</sup>. The total number of DOFs is 108 and just the 36 transitional DOFs (along the X- and Y-dimensions) are considered for OSP. The transitional DOFs corresponding to each node are shown in Table 12.

In this structure, the first 7 modes are employed for the OSP problem. The normal distribution characteristics for the uncertainty parameters are given in Table 13.

In this experimental test, the structure is instrumented with 18 triaxial piezo-electric accelerometers which are attached close to the 18 active nodes. A shaker mounted at node 18 is used to excite the structure along the X-direction as shown in Fig. 7(a). The excitation is considered as a Gaussian white noise sequence. The sampling rate of data acquisition is 6 kHz and 22 s long data were recorded for analysis. The modal properties of the structure are first identified using the Frequency Domain Decomposition (FDD) based on all the nodal measurement. Sun and Büyüköztürk (2015) carried out the OSP of 10 sensors for the experimental frame structure based on two objective function,  $f_1(\vartheta)$  and  $f_2(\vartheta)$ . The OSP for both cases are visualized in Table 14.

In this study, the probability of choosing each degree of freedom as one of the 10 positions of sensors is obtained from Fig. 8. Within these figures, 10 sensor positions with the highest probability are considered optimal, which are shown in Table 14.

According to Table 14, the OSPs obtained by the mentioned algorithms are similar in some DOFs. For each OSP obtained from Table 14, the three assessment criteria are evaluated according to Table 15.

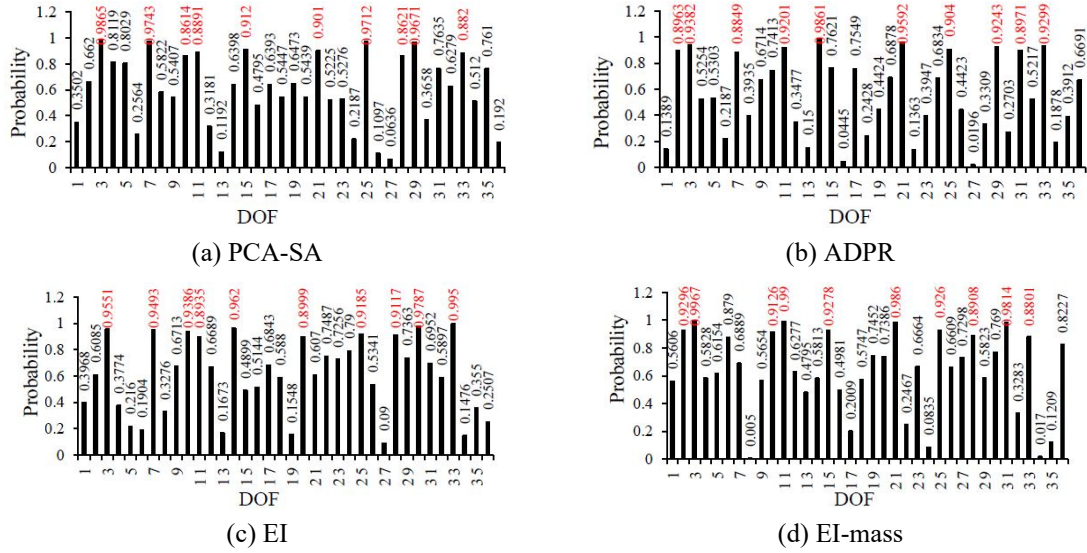


Fig. 8 Probability of the sensor placement

Table 14 DOFs corresponding to the optimal sensor placement

Algorithm	DOF				
PCA-SA	3	7	10	11	15
	21	25	28	29	33
ADPR	2	3	7	11	14
	21	25	29	31	33
EI	3	7	10	11	14
	20	25	2	30	33
EI-mass	2	3	10	11	15
	21	25	28	31	33
$f_1(\theta)$	2	3	7	10	11
(Sun and Büyüköztürk 2015)	12	14	21	25	29
$f_2(\theta)$	3	7	10	11	14
(Sun and Büyüköztürk 2015)	20	25	29	30	33

A comparison of FIM values in Table 15 indicates that the OSP obtained by the PCA-SA algorithm is more accurate than the other algorithms. The mentioned point reflects that the PCA-SA better maintains the linear independence between the mode shapes than the other algorithms. In this example, the RMS value in all algorithms is almost similar; although this criterion in PCA-SA algorithm is a bit lower than the other algorithms. Furthermore, the SVD value obtained by PCA-SA is higher than the other algorithms. Ultimately, the results of the proposed algorithm are suitable for OSP.

Table 15 Assessment criteria for the obtained sensor placement

Algorithm	Criteria		
	FIM	RMS	SVD
PCA-SA	5.4616	0.4082	0.197
ADPR	1.8741	0.4088	0.164
EI	2.4651	0.4094	0.109
EI-mass	4.9745	0.4092	0.117
$f_1(\theta)$ (Sun and Büyüköztürk 2015)	3.2484	0.04085	0.187
$f_2(\theta)$ (Sun and Büyüköztürk 2015)	1.8522	0.04086	0.174

## 7. Conclusions

In this study, a novel algorithm called PCA-SA is proposed for optimal sensor placement based on the minimum error rate in the structural damage detection process. The effect of uncertainty on the OSP is also studied. In this algorithm, modal data, PCA method and sensitivity analysis are employed. For this purpose, the effect of noise on the response of the sensors is initially reduced using the PCA method. Subsequently, the OSP is determined by reducing errors in the damage detection process based on sensitivity analysis. The results of this algorithm are compared with three other algorithms for OSP through numerical examples. The considered examples are a truss bridge, a space dome, and a double-layer grid. In these examples, the uncertainty is considered in the form of a normal Gaussian distribution on the geometric characteristics and materials, including Young's modulus, density, and the cross-sectional area of structural elements. The noise is also imposed on the recorded responses of the sensors. In addition, three numerical criteria are assessed to evaluate and compare the obtained OSP. The comparison between the algorithms has illustrated that the OSP obtained by the proposed algorithm (PCA-SA) more appropriately maintains the linear independence between the mode shapes compared to the other algorithms. In the PCA-SA algorithm, the off-diagonal elements of the FIM matrix are lower than the other algorithms, and the eigenvectors are uncorrelated. Ultimately, the results indicate that the proposed algorithm represents a higher accuracy for OSP purposes than the other mentioned algorithms.

## References

- Alkayem, N.F., Cao, M., Zhang, Y., Bayat, M. and Su, Z. (2018), "Structural damage detection using finite element model updating with evolutionary algorithm: a survey", *Neural Comput. Appl.*, **30**, 389-411. <https://doi.org/10.1007/s00521-017-3284-1>
- Altunisik, A.C., Sevim, B., Sunca, F. and Okur, F.Y. (2021), "Optimal sensor placements for system identification of concrete arch dams", *Adv. Concrete Construct., Int. J.*, **11**(5), 397-407. <https://doi.org/10.12989/acc.2021.11.5.397>
- Beygzadeh, S., Salajegheh, E., Torkzdeh, P., Salajegheh, J. and Naseralavi, S.S. (2014), "An improved genetic algorithm for optimal sensor placement in space structures damage detection", *Int. J. Space Struct.*, **29**(3), 121-136. <https://doi.org/10.1260/0266-3511.29.3.121>
- Castro-Triguero, R., Murugan, S., Gallego, R. and Friswell, M.I. (2013), "Robustness of optimal sensor placement under parametric uncertainty", *Mech. Syst. Signal Proc.*, **41**, 268-287.

- <https://doi.org/10.1016/j.ymsp.2013.06.022>
- Chisari, C., Macorini, L., Amadio, C. and Izzuddin, B.A. (2017), "Optimal sensor placement for structural parameter identification", *Struct. Multidiscip. Optim.*, **55**, 647-662.  
<https://doi.org/10.1007/s00158-016-1531-1>
- Das, S. and Dhang, N. (2022), "Damage identification of structures using incomplete mode shape and improved TLBO-PSO with self-controlled multi-stage strategy", *Structures*, **35**, 1101-1124.  
<https://doi.org/10.1016/j.istruc.2021.07.089>
- Dinh-Cong, D., Vo-Duy, T., Ho-Huu, V., Dang-Trung, H. and Nguyen-Thoi, T. (2017), "An efficient multi-stage optimization approach for damage detection in plate structures", *Adv. Eng. Soft.*, **112**, 76-87.  
<https://doi.org/10.1016/j.advengsoft.2017.06.015>
- Dinh-Cong, D., Dang-Trung, H. and Nguyen-Thoi, T. (2018), "An efficient approach for optimal sensor placement and damage identification in laminated composite structures", *Adv. Eng. Soft.*, **119**, 48-59.  
<https://doi.org/10.1016/j.advengsoft.2018.02.005>
- Ghannadi, P., Kourehli, S.S., Noori, M. and Altabey, W.A. (2020), "Efficiency of grey wolf optimization algorithm for damage detection of skeletal structures via expanded mode shapes", *Adv. Struct. Eng.*, **23**(13), 2850-2865. <https://doi.org/10.1177/1369433220921000>
- Ghiasi, R., Torkzadeh, P. and Noori, M. (2016), "A machine-learning approach for structural damage detection using least square support vector machine based on a new combinational kernel function", *Struct. Health Monitor.*, **15**, 302-316. <https://doi.org/10.1177/1475921716639387>
- Ghiasi, R., Fathnejat, H. and Torkzadeh, P. (2019), "A three-stage damage detection method for large-scale space structures using forward substructuring approach and enhanced bat optimization algorithm", *Eng. Comput.*, **35**, 857-874. <https://doi.org/10.1007/s00366-018-0636-0>
- He, L., Lian, J., Ma, B. and Wang, H. (2014), "Optimal multiaxial sensor placement for modal identification of large structures", *Struct. Control Health Monitor.*, **21**(1), 61-79. <https://doi.org/10.1002/stc.1550>
- Hosseini-Toudeshky, H. and Amjad, F.A. (2021), "Sensor placement optimization for guided wave-based structural health monitoring", *Struct. Monitor. Maint., Int. J.*, **8**(2), 125-150.  
<https://doi.org/10.12989/smm.2021.8.2.125>
- Hotelling, H. (1993), "Analysis of a complex of statistical variables into principal components", *J. Edu. Psych.*, **24**(6), 417-441. <https://doi.org/10.1037/h0071325>
- Kahya, V., Okur, F.Y., Karaca, S., Altunisik, A.C. and Aslan, M. (2021), "Multiple damage detection in laminated composite beams using automated model update", *Structures*, **34**, 1665-1683.  
<https://doi.org/10.1016/j.istruc.2021.08.117>
- Kammer, D.C. (1991), "Sensor placement for on-orbit modal identification and correlation of large space structures", *J. Guid. Control Dyn.*, **14**(2), 251-259. <https://doi.org/10.2514/3.20635>
- Kammer, D.C. and Peck, J.A. (2008), "Mass-weighting methods for sensor placement using sensor set expansion techniques", *Mech. Syst. Signal Process.*, **22**(7), 1515-1525.  
<https://doi.org/10.1016/j.ymsp.2008.01.002>
- Kaveh, A. and Zolghadr, A. (2015), "An improved CSS for damage detection of truss structures using changes in natural frequencies and mode shapes", *Adv. Eng. Soft.*, **80**, 93-100.  
<https://doi.org/10.1016/j.advengsoft.2014.09.010>
- Khatir, S., Wahab, M.A., Boutchicha, D. and Khatir, T. (2019), "Structural health monitoring using modal strain energy damage indicator coupled with teaching-learning-based optimization algorithm and isogoemetric analysis", *J. Sound Vib.*, **448**, 230-246. <https://doi.org/10.1016/j.jsv.2019.02.017>
- Kim, T., Youn, B.D. and Oh, H. (2018), "Development of a stochastic effective independence (SEFI) method for optimal sensor placement under uncertainty", *Mech. Syst. Signal Proc.*, **111**, 615-627.  
<https://doi.org/10.1016/j.ymsp.2018.04.010>
- Laory, I., Hadj Ali, N.B., Trinh, T.N. and Smith, I.F.C. (2012), "Measurement system configuration for damage identification of continuously monitored structures", *J. Bridge Eng.*, **17**(6), 857-866.  
[https://doi.org/10.1061/\(ASCE\)BE.1943-5592.0000386](https://doi.org/10.1061/(ASCE)BE.1943-5592.0000386)
- Liu, K., Yan, R.J. and Soares, C.G. (2018), "Optimal sensor placement and assessment for modal identification", *Ocean Eng.*, **165**, 209-220. <https://doi.org/10.1016/j.oceaneng.2018.07.034>

- Liu, C., Teng, J. and Peng, Z. (2020), "Optimal sensor placement for bridge damage detection using deflection influence line", *Smart Struct. Syst., Int. J.*, **25**(21), 169-181.  
<https://doi.org/10.12989/sss.2020.25.2.169>
- Lofrano, E., Pingaro, M., Trovalusci, P. and Paolone, A. (2020), "Optimal sensor placement in dynamic damage detection of beam using a statistical approach", *J. Optim. Theory Appl.*, **187**, 758-775.  
<https://doi.org/10.1007/s10957-020-01761-3>
- Naseralavi, S.S., Salajegheh, J., Salajegheh, E. and Fadaei, M.J. (2010), "An improved genetic algorithm using sensitivity analysis and micro search for damage detection", *Asian J. Civil Eng.*, **11**(6), 717-740.
- Ostachowicz, W., Soman, R. and Malinowski, P. (2019), "Optimization of sensor placement for structural health monitoring: A review", *Struct. Health Monitor.*, **18**(3), 963-988.  
<https://doi.org/10.1177/1475921719825601>
- Pearson, K. (1901), "LIII. On lines and planes of closest fit to systems of points in space", *The London, Edinburgh, and Dublin Philosophical Magazine and Journal of Science*, **2**(6), 559-572.  
<https://doi.org/10.1080/14786440109462720>
- Pourali, M. and Mosleh, A. (2013), "A bayesian approach to sensor placement optimization and system reliability monitoring", *J. Risk Reliable.*, **227**(3), 327-347. <https://doi.org/10.1177/1748006X13485663>
- Rao, A.R.M., Lakshmi, K. and Krishnakumar, S. (2014), "A generalized optimal sensor placement technique for structural health monitoring and system identification", *Procedia Eng.*, **86**, 529-538.  
<https://doi.org/10.1016/j.proeng.2014.11.077>
- Robert, C.P. and Casella, G. (2010), *Monte Carlo Statistical Methods*, (2nd Edition), Springer, New York.
- Shi, Q., Wang, X., Chen, W. and Hu, K. (2020), "Optimal sensor placement method considering the importance of structural performance degradation for the allowable loadings for damage identification", *Appl. Math. Model.*, **86**, 384-403. <https://doi.org/10.1016/j.apm.2020.05.021>
- Shyamala, P., Mondal, S. and Chakraborty, S. (2018), "Numerical and experimental investigation for damage detection in FRP composite plates using support vector machine algorithm", *Struct. Monitor. Maint., Int. J.*, **5**(2), 243-260. <https://doi.org/10.12989/smm.2018.5.2.243>
- Sun, H. and Büyüköztürk, O. (2015), "Optimal sensor placement in structural health monitoring using discrete optimization", *Smart Mater. Struct.*, **24**(12), 125034.  
<https://doi.org/10.1088/0964-1726/24/12/125034>
- Tan, Y. and Zhang, L. (2020), "Computational methodologies for optimal sensor placement in structural health monitoring: A review", *Struct. Health Monitor.*, **19**(4), 1287-1308.  
<https://doi.org/10.1177/1475921719877579>
- Vincenzi, L. and Simonini, L. (2017), "Influence of modal errors in optimal sensor placement", *J. Sound Vib.*, **389**, 119-133. <https://doi.org/10.1016/j.jsv.2016.10.033>
- Wang, J. and Yang, Q.S. (2017), "Sensor selection approach for damage identification based on response sensitivity", *Struct. Monitor. Maint., Int. J.*, **4**(1), 53-68. <https://doi.org/10.12989/smm.2017.4.1.053>
- Yang, Ch., Lu, Z. and Yang, Z. (2018), "Robust optimal sensor placement for uncertain structures with interval parameters", *IEEE Sensors J.*, **18**(5), 2031-2041. <https://doi.org/10.1109/JSEN.2018.2789523>
- Yi, T.H., Li, H.N., Song, G. and Zhang X.D. (2015), "Optimal sensor placement for health monitoring of high-rise structure using adaptive monkey algorithm", *Struct. Cont. Health Monitor.*, **22**(4), 667-681.  
<https://doi.org/10.1002/stc.1708>
- Yi, T.H., Zhou, G.D., Li, H.N. and Wang, C.W. (2017), "Optimal placement of triaxial sensor for modal identification using hierarchic wolf algorithm", *Struct. Cont. Health Monitor.*, **24**(8), e1958.  
<https://doi.org/10.1002/stc.1958>
- Zhang, J., Maes, K., De Roeck, G., Reynders, E., Papadimitriou, C. and Lombaert, G. (2017), "Optimal sensor placement for multi-setup modal analysis of structures", *J. Sound Vib.*, **401**, 214-232.  
<https://doi.org/10.1016/j.jsv.2017.04.041>
- Zhang, G., Tang, L., Zhou, L., Liu, Z., Liu, Y. and Jiang, Z. (2019), "Principal component analysis method with space and time windows for damage detection", *Sensors*, **19**(11), 1-23.  
<https://doi.org/10.3390/s19112521>
- Zhou, G.D., Yi, T.H., Zhang, H. and Li, H.N. (2015a), "Energy-aware wireless sensor placement in

- structural health monitoring using hybrid discrete firefly algorithm”, *Struct. Health Monit.*, **22**(4), 648-666.  
<https://doi.org/10.1002/stc.1707>
- Zhou, G.D., Yi, T.H., Zhang, H. and Li, H.N. (2015b), “Optimal sensor placement under uncertainties using a nondirective movement glowworm swarm optimization algorithm”, *Smart Struct. Syst., Int. J.*, **16**(2), 243-262. <https://doi.org/10.12989/sss.2015.16.2.243>
- Zhou, G.D., Xie, M.X., Yi, T.H. and Li, H.N. (2019), “Optimal wireless sensor network configuration for structural monitoring using automatic-learning firefly algorithm”, *Adv. Struct. Eng.*, **22**(4), 907-918.  
<https://doi.org/10.1177/1369433218797074>

*HL*